Chapter 3

Recovery of copper from metallic fraction of WPCBs of end-of-life computer motherboards

3. Recovery of copper from metallic fraction of WPCBs of end-of-life computer motherboards

This chapter outlines the development of a leaching technique aimed at achieving the highest possible retrieval of copper, zinc, and nickel from the metal clads found in outdated computer motherboards' PCBs. To extract copper from a concentrate abundant in metals, acid leaching was utilized. Subsequent experiments focused on refining the leaching process by optimizing various factors such as temperature, leaching duration, leachant strength, and pulp density. Additionally, the chapter presents findings from kinetic studies, including the calculation of experimental activation energies. These energies were determined as part of investigating the reaction mechanism involved in the dissolution of copper and zinc during the leaching process.

3.1. Characterization of WPCBs of obsolete computer motherboards

Printed circuit boards have complex compositions as they are made of multiple layers, all stacked up into a sandwich-like structure. For a better understanding of the structure of PCB, the cross-sectional study was done. To achieve this, we cut a 0.5x0.5 cm^2 size of PCB part and attached two such parts to support the mounting process of this sample onto the sample holder. This 0.5x0.5 cm^2 PCB piece was mounted on the SEM sample holder with the help of carbon tape and subjected to SEM, EDX, and elemental mapping studies.

A zoom-in image of the PCB section is shown in Figure 3.1(c). We can see distinct layers in the PCB. There is an external coating, fiberglass layer, and Cu-rich metallic layer, followed by more fiberglass layers. All the layers are joined together by epoxy resin. This has been further confirmed by the EDX. Each layer underwent EDX spectrum collection to determine its composition. The corresponding EDX findings are marked in *Figure 3.2.*

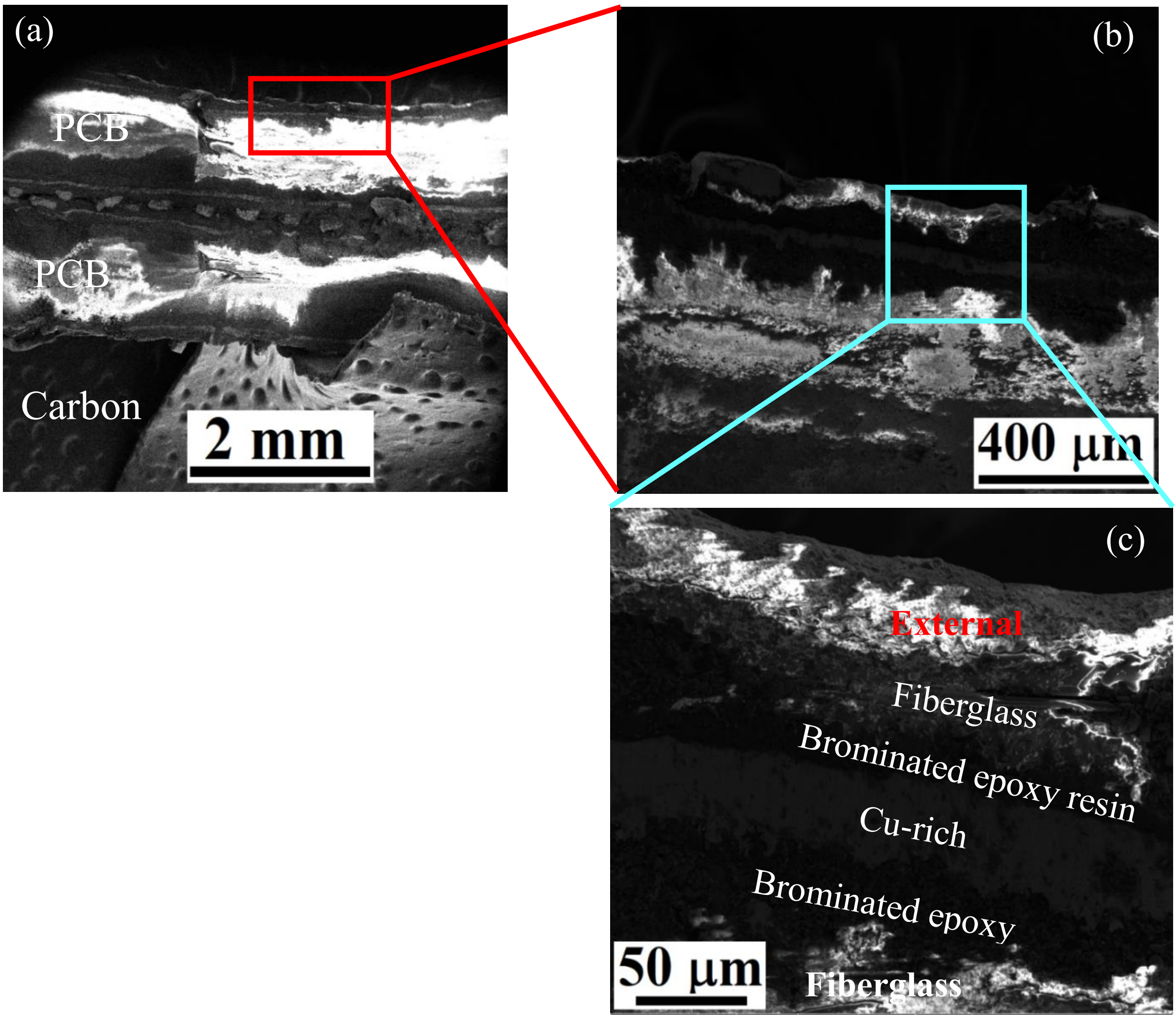

Figure 3.1 (a) Low magnification image showing cross-section of PCB, (b,c) zoomed-in image to show the distinct layers present in the PCB

From *Figure 3.2(a)* we can see that the top resin layer of bare PCB which is commonly green or blue colour is rich in C, O, and S forming the protective coating on the epoxy resin, which protects the circuit board from corrosion. It is coated on a fiberglass layer so it shows the presence of Al, Si, Ba. Sn and Pb are elements of solders for connections between the electrical components and board. EDX from the other layer (*Figure 3.2(b)*) shows the presence of Al, Si, Mg, Ca, and Ba denoting that the fiberglass layer is made of Al_2O_3, SiO_2, MgO, CaO, and BaO.

Fe and Cu are present in the tracks and wires forming a conductive connection between the layers. EDX of this region shows the presence of C, O, and Br from brominated epoxy resin. EDX of metallic layer embedded between the fiberglass layers (Figure 3.2(c)) shows Cu richness along with very small weight% of Zn, Ni, and Fe. There are multiple glassfiber layers between the two metallic layers (*Figure 3.2(b,d)*).

Figure 3.3 shows the elemental map of the cross-section of PCB. Distinct element distribution is clearly seen. C, O, Br are present in the organic used in epoxy resin. Cu, Ni, Zn, and Fe are the construction elements in the metallic layer. Sn is present in the solder material. Si, Al, Ca, Mg, and Ba are the non-metals used in construction of fiberglass layers and are present as SiO_2, Al_2O_3, CaO, MgO, and BaO. This has been further confirmed with various literatures (Li et al., 2018; Szalatkiewicz Jakub, 2014; Tatariants et al., 2018).

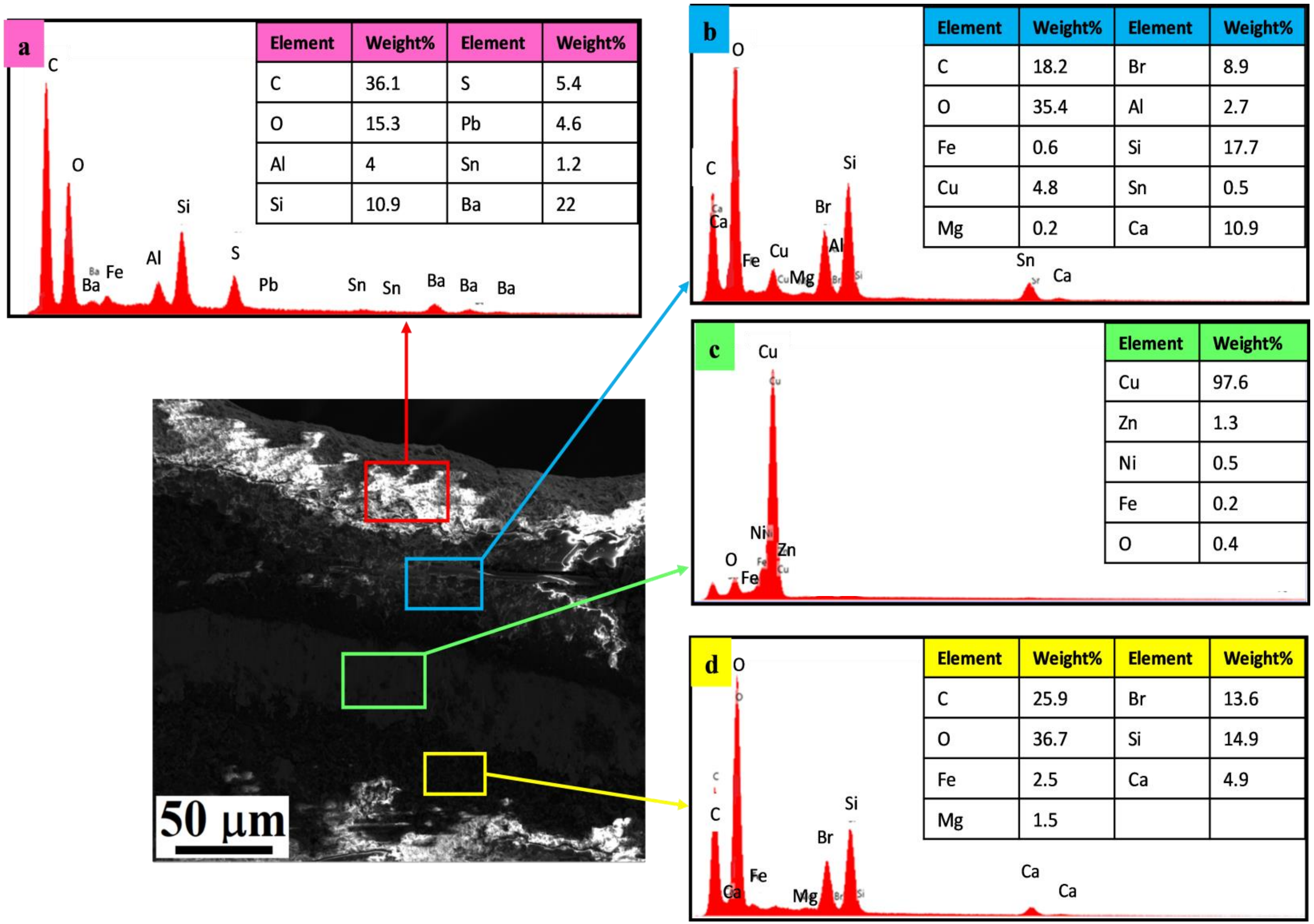

a

Element	Weight%	Element	Weight%
C	36.1	S	5.4
O	15.3	Pb	4.6
Al	4	Sn	1.2
Si	10.9	Ba	22

b

Element	Weight%	Element	Weight%
C	18.2	Br	8.9
O	35.4	Al	2.7
Fe	0.6	Si	17.7
Cu	4.8	Sn	0.5
Mg	0.2	Ca	10.9

c

Element	Weight%
Cu	97.6
Zn	1.3
Ni	0.5
Fe	0.2
O	0.4

d

Element	Weight%	Element	Weight%
C	25.9	Br	13.6
O	36.7	Si	14.9
Fe	2.5	Ca	4.9
Mg	1.5		

Figure 3.2 EDX of the different layers of the cross-section of WPCB-motherboard (a) top resin layer (b) fiberglass (c) metallic layer (d) fiberglass layer

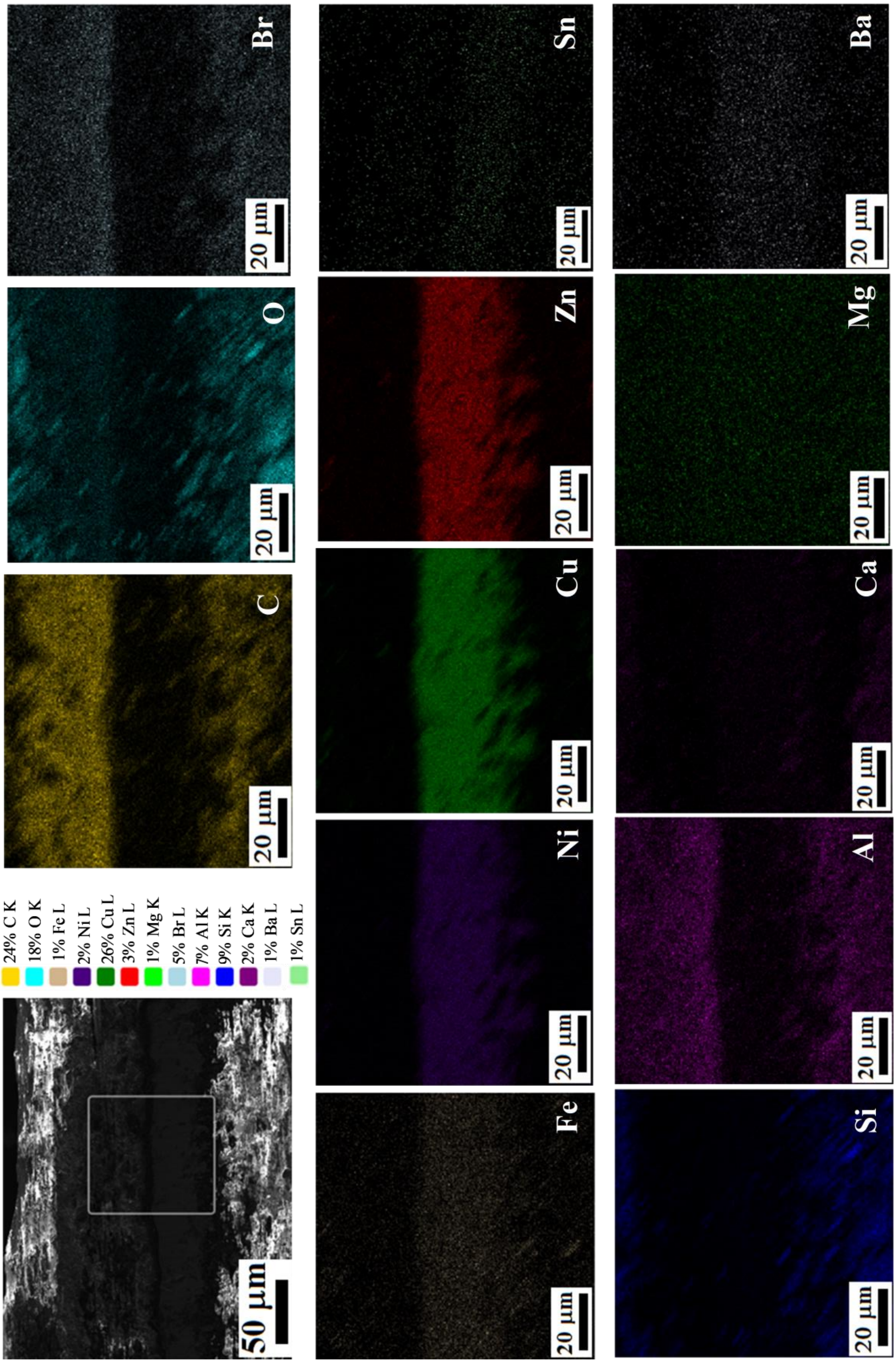

Figure 3.3 Elemental mapping of the cross-section of PCB

3.2. Recovery of copper from metallic fraction of computer motherboard PCBs

3.2.1. Nitric acid leaching

The metal fraction generated during the pre-treatment process is dissolved in different nitric acid solutions to assess the leaching effectiveness. To achieve the highest extraction of metallic values from the metal sheets into the solution, the leaching conditions with nitric acid were fine-tuned to optimize the recovery of copper and zinc. Potentiometric leaching/polarization study depends on pH of the solution. Potential is affected by pH change, as the concentration of Cu^{2+} decreases (Bralić et al., 2014). To administer the pH suitable for copper dissolution, potential change of the electrochemical system is inevitable which leads to formation of passive film on the surface of WPCB metal clads, hence lowering the dissolution rate observed during potentiometric leaching. Further to maintain the pH of the solution, the addition of acid or base would be needed which would change the concentration of solution, hence decreasing the dissolution of copper and reducing the concentration of Cu^{2+} (Mbuyi et al., 2014). The drop in the potential is due to formation of $Cu(OH)_x$ complexes which decreases the “free Cu^{2+}”, thus lowering the Cu^{2+} concentration (Bralić et al., 2014). Hence in our case we did not perform potentiometric leaching to avoid obtaining wrong detected values of the copper concentration detected by AAS.

Use of Response Surface Methodology (RSM), a statistical modelling technique to study the effect of parameter optimization has already been reported for HNO_3 leaching media reagents for copper recovery (Rao et al., 2021a; Vijayaram and Chandramohan, 2013). So experimental studies were performed in detail to optimize the parameters by triplicating the experiments.

i) Effect of concentration of nitric acid

Three separate leaching trials were performed, varying the concentration of nitric acid from 1 to 3 M, maintaining a temperature of 30ºC, a duration of 3 h, a pulp density of 50 g/L, and a stirring speed of 500 rpm. Increasing the acid concentration from 1 to 3 M demonstrated a progressive rise in copper and zinc content within the leach solution (as seen in *Figure 3.4 (a) and (b)*). Complete leaching of copper and zinc was achieved notably using 3 M nitric acid within 2 h. Accordingly, employing 3 M nitric acid for a duration of 2 h emerges as the most efficient approach for effectively leaching copper and zinc.

ii) Effect of temperature

The impact of temperature on the dissolution of copper and zinc was investigated by varying it from 30 to 60°C, maintaining the optimized nitric acid concentration (3M) and time duration (2 hours). Additional factors such as 50 g/L pulp density and a stirring speed of 500 rpm were held constant. The findings indicate that, the leaching of copper and zinc intensifies as temperature increases (upto 40ºC), leading to 99.9% leaching efficiency of Cu and 99.3% for Zn. This is attributed to the increased acceleration of the thermal motion of molecules and the increased surface contact between particles because of increased kinetic energy from heating (Godirilwe et al., 2021). Above 50ºC, there's a decline in the dissolution of Cu (as shown in Figure 3.5(a) and (b)), likely attributed to metal hydrolysis. Elevated temperatures lead to increased acid loss through volatilization. Consequently, the metal interacts with water, entering the residue and consequently hindering further dissolution reactions (Zhang et al., 2016). Moreover, at temperature of 60ºC, the leaching process exhibited rapid kinetics within the first 60 minutes (with Cu leaching efficiency of 95.2%), followed by a deceleration in reaction speed upto 120 min leaching time (reducing the leaching efficiency to 85.3%), as shown in Figure 3.5(a). This was further confirmed by dissolving the residue obtained at 60°C in aqua regia. The AAS results of the dissolved residue showed 0.103% Cu in the solution. So we confirmed that Cu has entered the residue causing reduction in leaching efficiency at elevated temperature. Hence, it was concluded that the optimal conditions for maximizing leaching efficiency were a temperature of 30ºC and a leaching duration of 120 minutes which saves energy and avoides vaporization of the nitric acid solution.

iii) Effect of pulp density

The pulp density was varied from 25-100 g/L to evaluate its impact on the leaching efficiency of metals. Other parameters (3 M HNO_3, 30ºC, 120 min, 500 rpm) were kept same. As the pulp density increased, there was a gradual rise in the dissolution of Cu and Zn. However, the dissolution of Cu started to decrease at higher pulp densities (above 75 g/L) as shown in *Figure 3.6(a) and (b)*, likely due to inefficient mass transfer and a reduction in residual acid concentration, in line with findings from earlier studies (Chen et al., 2015; Kumar et al., 2014). As the S/L ratio increases above 50 g/L, the slurry density gradually increases, decelerating mass transfer, and therefore negatively affecting the metalclad dissolution, hence decreasing the Cu leaching efficiency. Also the increase in S/L ratio increases the quantity of non-metallic materials, promoting the agglomeration of raw materials, causing collisions and frictions between the metal clads during the leaching process, which would impede the full contact of metals with leaching solutions, thereby reducing the leaching efficiency. In addition, the contents of active metals (Pb, Sn, Fe, Ni, Zn) increase in the raw materials with the increase in S/L ratio, which reduces copper ions in the leaching solution through replacement reactions, hence reducing the leaching efficiency of Cu (Hao et al., 2022). Therefore, the optimum S/L ratio was 50 g/L. Since increasing the volume of leaching solution increases the efficiency of mass transfer, copper recovery is accelerated (Chen et al., 2015). Hence, to ensure the complete dissolution of both metals, a pulp density of 50 g/L was selected for subsequent experiments.

iv) Effect of stirring speed

In the final phase, the stirring speed was adjusted within the range of 100-500 rpm while maintaining 3 M nitric acid, a 2 h residence time, 30ºC, and a pulp density of 50 g/L. The leaching of Cu and Zn showed a slight increase with higher stirring speeds. At lower speeds the WPCB metalclads donot suspend completely and the heavier metal particles are deposited at the bottom of the beaker, thereby hindering full contact of the metal with the leaching reagent, hence decreasing the leaching efficiency. Increasing the stirring speed will promote the suspension of metalclads, decreasing the thickness of mass transfer boundary layer on the surface of the particles (Bayati et al., 2018). In kinetic terms, a higher stirring speed accelerates the diffusion rate of the metal particles in the leaching solution and enables homogeneous mixing of the solid and liquid phases in the reactor vessel, which can promote the reaction, hence increasing the leaching efficiency (Clotilde Apua and Madiba, 2021; Deng et al., 2015). However, speeds exceeding 500 rpm resulted in significant acid splashing, causing metallic materials to adhere to the upper reactor walls. It also forms air pockets in the liquid at the interface, thus reducing the rate of dissolution of Cu. Therefore, 500 rpm was deemed the optimal stirring speed for effective leaching. Maximum Cu leaching efficiency (99.9%) and Zn leaching efficiency (99.3%) is obtained at stirring speed of 500 rpm after 120 min. At 400 rpm the leaching efficiency of Cu and Zn after 120 min is 92% and 99.3%. So we have chosen 500 rpm as the optimal stirring speed to get maximum recovery of the major element of interest i.e. Cu. At this stirring speed maximum recovery of other elements such as zinc and nickel is also obtained.

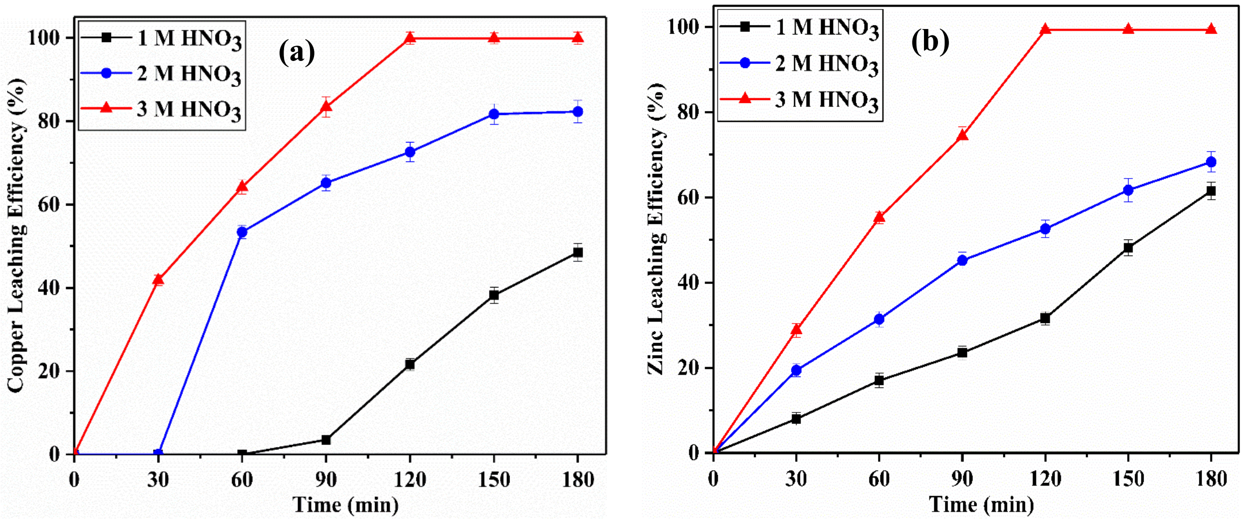

Figure 3.4 Effect of concentration of nitric acid on (a) copper, (b) zinc [Temp. 30°C; time 3 h; stirring speed 500 rpm; pulp density 50 g/L]

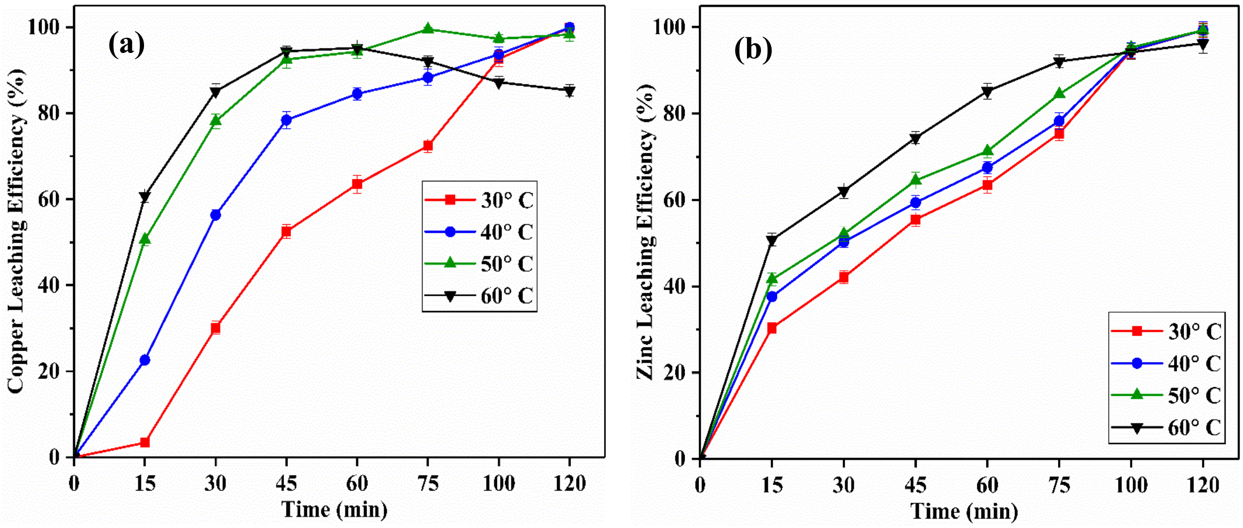

Figure 3.5 Effect of temperature on nitric acid leaching of (a) copper, (b) zinc [Concentration of nitric acid 3 M; time 3 h; stirring speed 500 rpm; pulp density 50 g/L]

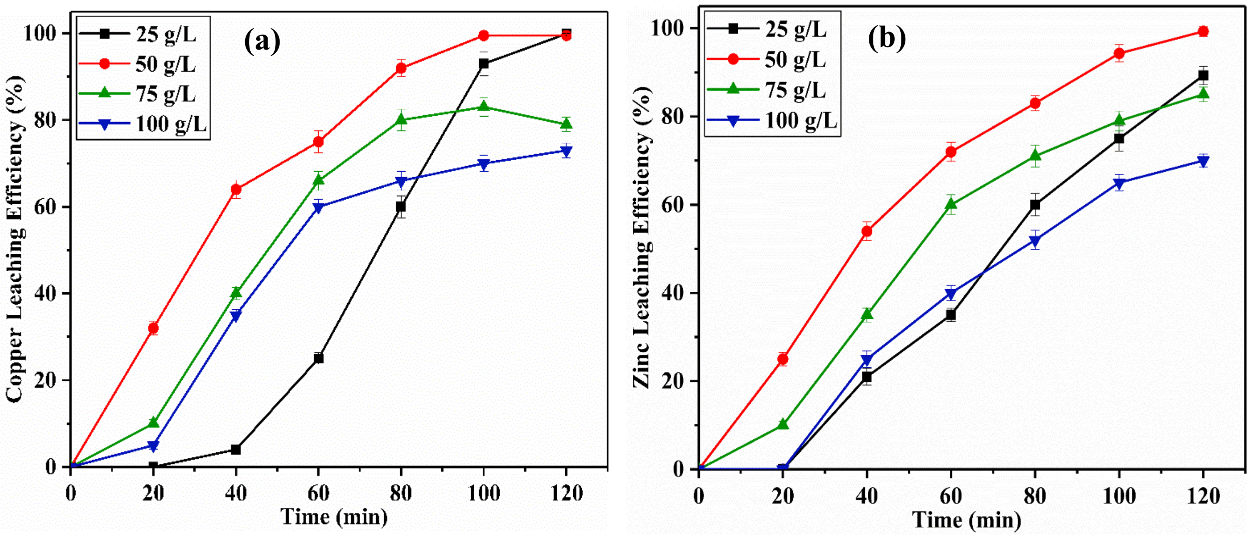

Figure 3.6 Effect of pulp density on nitric acid leaching of (a) copper, (b) zinc
[Concentration of nitric acid 3 M; temp. 30°C; time 2 h; stirring speed 500 rpm]

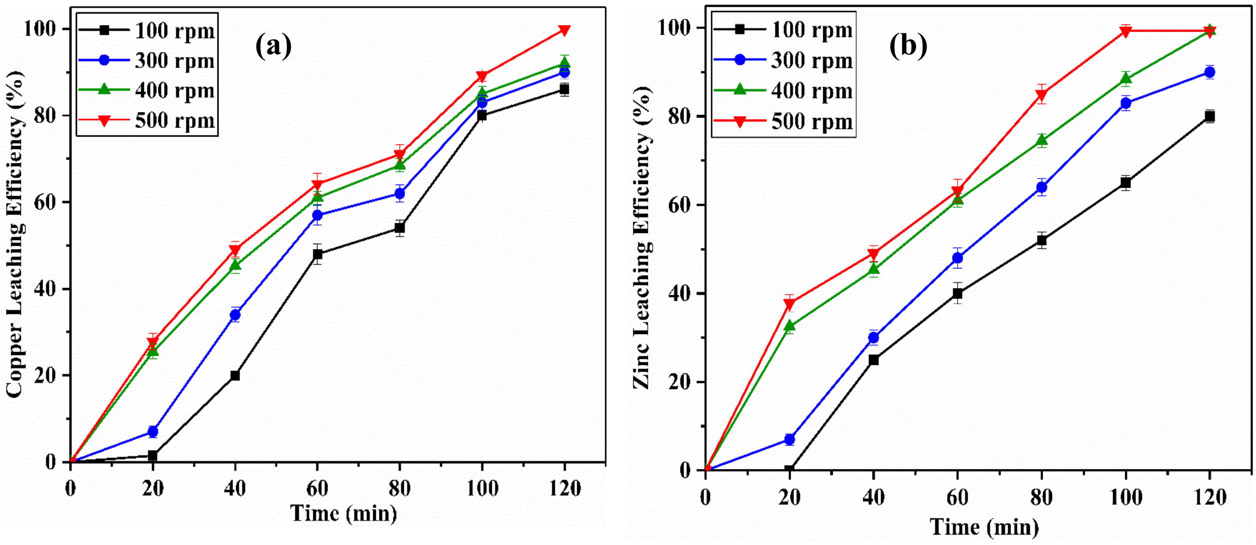

Figure 3.7 Effect of pulp density on nitric acid leaching of (a) copper, (b) zinc
[Concentration of nitric acid 3 M; temp. 30°C; time 2 h; pulp density 50 g/L]

The optimized parameters for efficiently leaching copper and zinc involve using 3M nitric acid, maintaining a temperature of 30°C, a residence time of 2 hours, a pulp density of 50 g/L, and an agitation speed of 500 rpm. These optimized conditions not only facilitate the dissolution of copper (99.9%) and zinc (99.3%) but also result in the dissolution of nickel (99.0%), as depicted in *Figure 3.8*. Throughout this process, higher concentrations of nitric acid led to the substantial generation of NO_x gases, as demonstrated in *Eq. 3.1-3.4*. To maintain environmental sustainability, these gases would need to be scrubbed and reintegrated into fresh nitric acid. Scrubbing has not been extensively studied in the current thesis. Scrubbing of NO_x gas and regeneration of nitric acid study has been reported by Dry and Harris. NO_x vapor is retained in nitric acid regeneration system, which is a series of adsorbers and scrubbers, and was reacted with HNO_3. Afterwards it was allowed to oxidize with air and cooled to condense as nitric acid. Therefore, 99% of the NO_x was recovered to form a 55% nitric acid. The nitric acid regeneration reaction sequence is given in *Eq. 3.5-3.10* (Dry and Harris, 2012):

$$Cu + 4HNO_3 \rightarrow Cu(NO_3)_2 + 2H_2O + 2NO_2 \quad (3.1)$$

$$3Cu + 8HNO_3 \rightarrow 3Cu(NO_3)_2 + 4H_2O + 2NO \quad (3.2)$$

$$Zn + 4HNO_3 \rightarrow Zn(NO_3)_2 + 2H_2O + 2NO_2 \quad (3.3)$$

$$Ni + 4HNO_3 \rightarrow Ni(NO_3)_2 + 2H_2O + 2NO_2 \quad (3.4)$$

$$2NO + O_2 = 2NO_2 \quad (3.5)$$

$$3NO_2 + H_2O = 2HNO_3 + NO \quad (3.6)$$

$$4NO + 2HNO_3 = 2N_2O_3 + H_2O \quad (3.7)$$

$$N_2O_3 + O_2 + H_2O = 2HNO_3 \quad (3.8)$$

Overall stoichiometry:

$$NO + O_2 \rightarrow 2NO_2 \quad (3.9)$$

$$4NO_2 + H_2O + O_2 \rightarrow 4HNO_3 \quad (3.10)$$

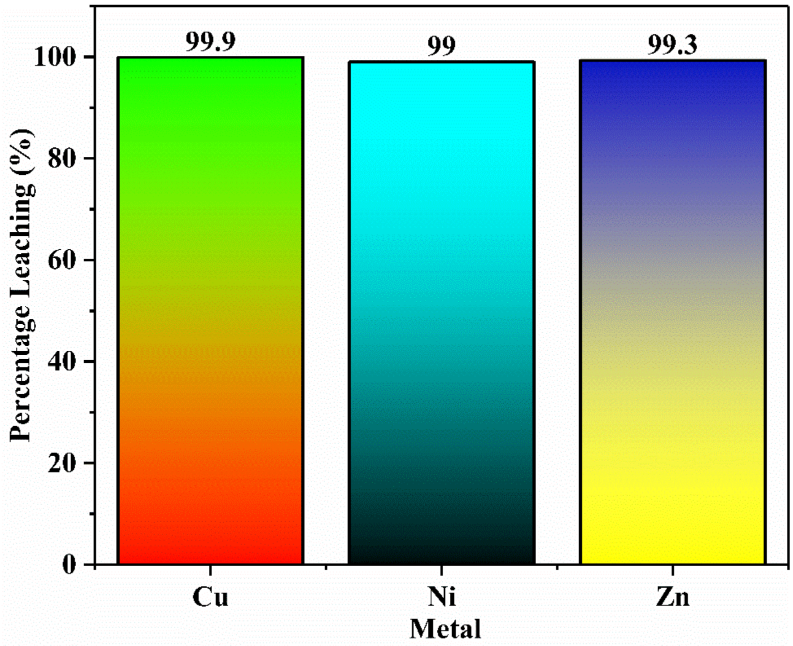

Figure 3.8 Leaching efficiency of various metals in nitric acid leaching [Concentration of nitric acid 3 M; temperature 30°C; time 2 h; stirring speed 500 rpm; pulp density 50 g/L]

At the optimized parameters, the chemical analysis of the filtered leachate indicated a composition of 98 ± 1 wt% copper and 0.57 ± 0.1 wt% zinc. Additionally, minor quantity of nickel (0.149 ± 0.2 wt%), was observed, as depicted in *Figure 3.9*.

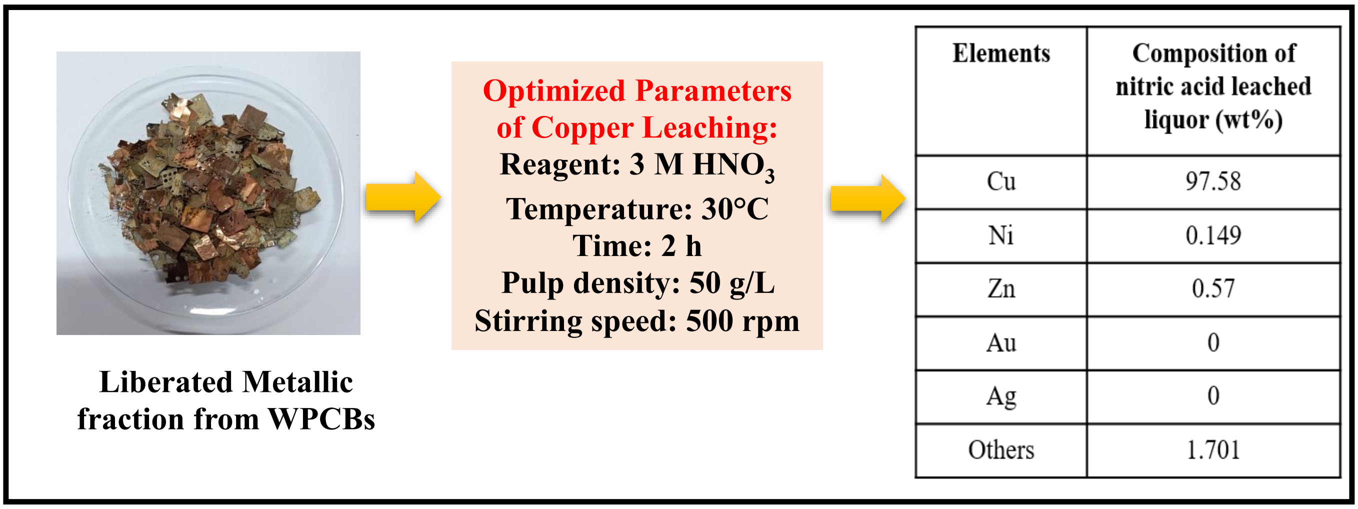

Elements	Composition of nitric acid leached liquor (wt%)
Cu	97.58
Ni	0.149
Zn	0.57
Au	0
Ag	0
Others	1.701

Figure 3.9 Chemical analysis of nitric acid leached solution obtained at optimized leaching parameters

3.2.2. Analysis of residue obtained after nitric acid leaching

SEM-EDX analysis of the separated residue, illustrated in *Figure 3.10*, reveals a predominant non-metallic fraction alongside the presence of tin.

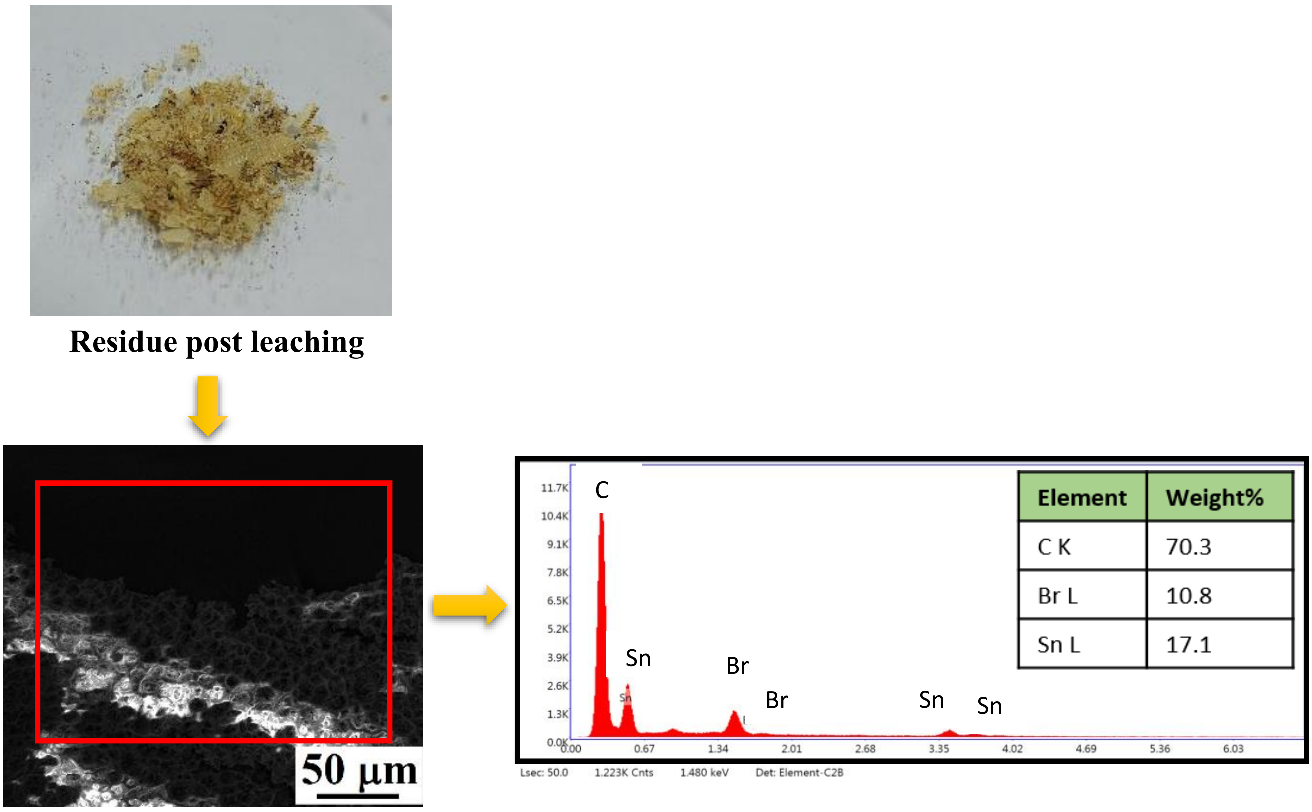

Element	Weight%
C K	70.3
Br L	10.8
Sn L	17.1

Figure 3.10 SEM-EDX of leach residue obtained in nitric acid leaching

3.2.3. Kinetics of dissolution of copper and zinc

Studying the rate of leaching is crucial for examining how copper and zinc dissolve from the separated metal layers of WPCBs. This exploration aids in grasping how the solid and liquid components interact differently at the solid-liquid boundary, shedding light on the heterogeneous interaction mechanism between the leachant and the solid feed (Wang et al., 2017; Wu et al., 2020). During leaching, the leaching reagent undergoes a series of consecutive reactions with mineral particles. These steps include:

a) Diffusion of the reagent from the bulk liquid phase to the porous boundary film
b) Diffusion of the reagent through the porous layer
c) Reaction of the reagent with the mineral surface, resulting in the creation of new products
d) Diffusion of the resulting metal product through the porous layer
e) Diffusion of the product metal away from the surface

The rate at which leaching occurs in a heterogeneous reaction model can be established using either the widely used shrinking core/sphere model or the Avrami model (Martínez-Luévanos et al., 2011; Wang et al., 2017). Within the shrinking core model (as per *Eq (3.5)*), the slowest step determining the rate involves the diffusion of reacting substances across the porous product layer. In contrast, the shrinking sphere model (in *Eq (3.6)*) identifies the surface chemical reaction as the step that sets the pace for the rate (Behera and Parhi, 2016). To ascertain the kinetic characteristics of the copper and zinc leaching reaction, the application of the shrinking core/sphere model involved analysing the variations in experimental percentage leaching over time at various temperatures, as depicted in *Figure 3.5*.

If the reaction is governed by the diffusion across the product layer, then *Eq (3.11)* remains valid (Olanipekun, 2000),

$$1 - \left(\frac{2}{3}\right)x - (1-x)^{2/3} = k_d t \qquad (3.11)$$

However, if the reaction is chemically controlled by a surface reaction, *Eq (3.12)* applies instead (Agacayak and Taner, 2019),

$$1 - (1-x)^{1/3} = k_c t \qquad (3.12)$$

Here, x represents the fraction of leaching, k_d stands for the kinetic rate constant governing the diffusion-controlled reaction, k_c represents the kinetic rate constant governing the surface reaction-controlled reaction, and t denotes the reaction time in minutes.

The information was utilized to fit data with both models, aiming to establish the kinetic model for this study, as depicted in *Figure 3.11*.

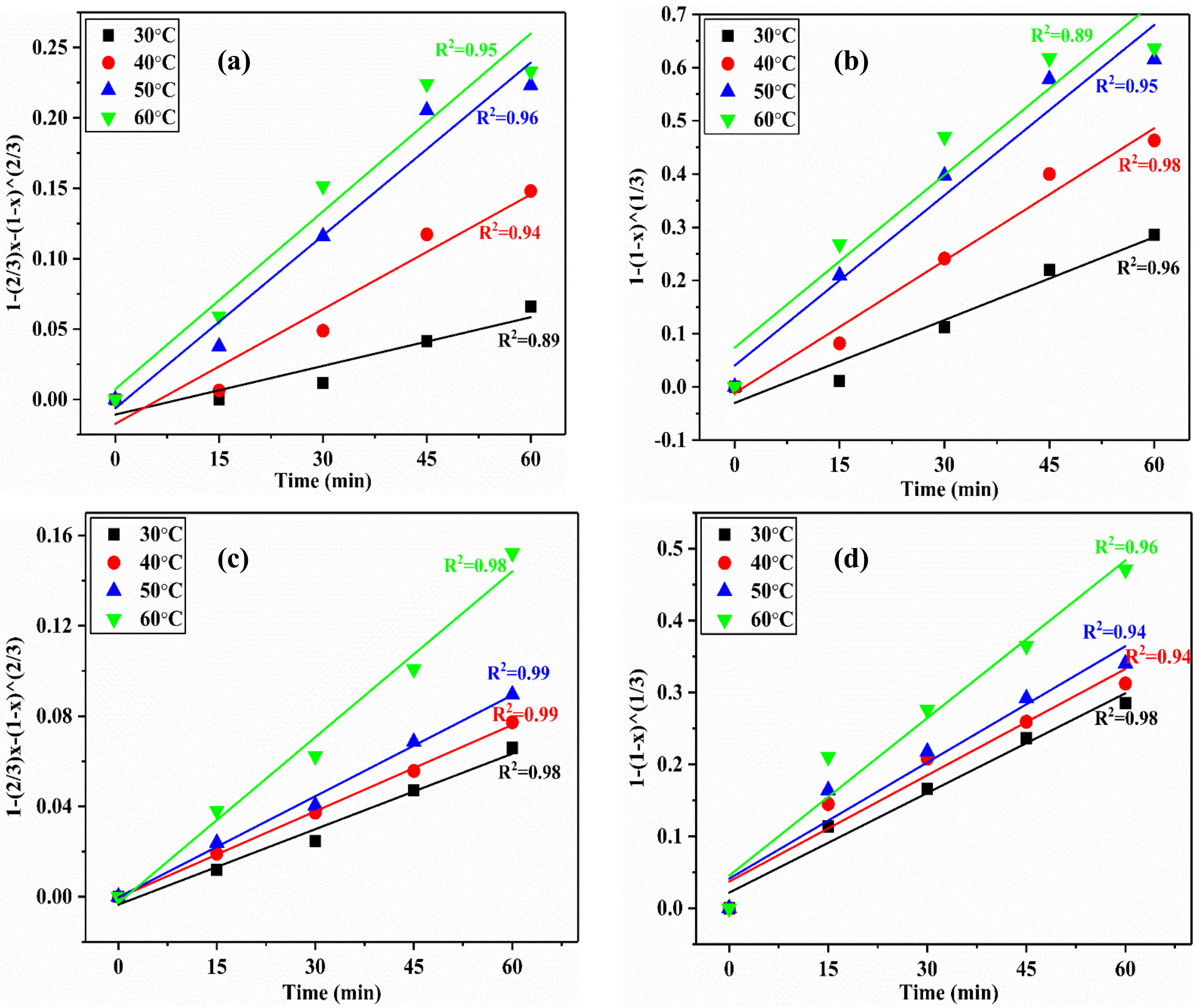

Figure 3.11 Kinetics plots for leaching of copper for (a) diffusion-controlled model and (b) reaction-controlled model and leaching of zinc for (c) diffusion-controlled model and (d) reaction-controlled model

Figure 3.11 depicts the kinetic plot, indicating a slightly superior fit for copper in the reaction-controlled process model ($R^2 \geq 0.94$) (*Figure 3.11a & b*). Conversely, zinc's kinetic data fits best with a diffusion-controlled model, showcasing a notably strong correlation ($R^2 \geq 0.98$) in *Figure 3.11c & d*.

The reaction rate constants, k_d and k_c, were derived from the slope observed in the linear correlation depicted in *Figure 3.11* using the Arrhenius equation (*Eq. 3.13*). This equation served to establish the link between these particular rate constants and temperature (shown in *Figure 3.12*), as demonstrated by:

$$k = Ae^{(-Ea/RT)} \tag{3.13}$$

where k is the rate constant, A is the pre-exponentiaal factor, E_a is the activation energy, and R is the gas constant (8.314 J K^{-1} mol^{-1}).

There is not much difference seen in the R^2 values in Figure 3.12. In Figure 3.12(a,b) we found R^2 to determine the slope values to calculate the activation energy. Hence we fit a straight line. However, other aspects of the plot were not part of our current study as it was not required. Linear fitting to calculate activation energy has been reported in other literatures (Agrawal et al., 2022; Rao et al., 2021b). Activation energy less than 20 kJ/mol suggests that the controlling step is diffusion, more than 40 kJ/mol corresponds to chemical reaction control and a value in between implies that mixed mechanism affect the rate of leaching (Faraji et al., 2020). In our scenario, the calculated activation energy for copper leaching from diffusion and reaction control mechanism stood at 37.20 and 23.04 kJ/mol, and for zinc leaching it was found to be 23.02 and 9.16 kJ/mol, respectively. These values strongly favor the proposed leaching mechanism being governed by a mixed mechanism.

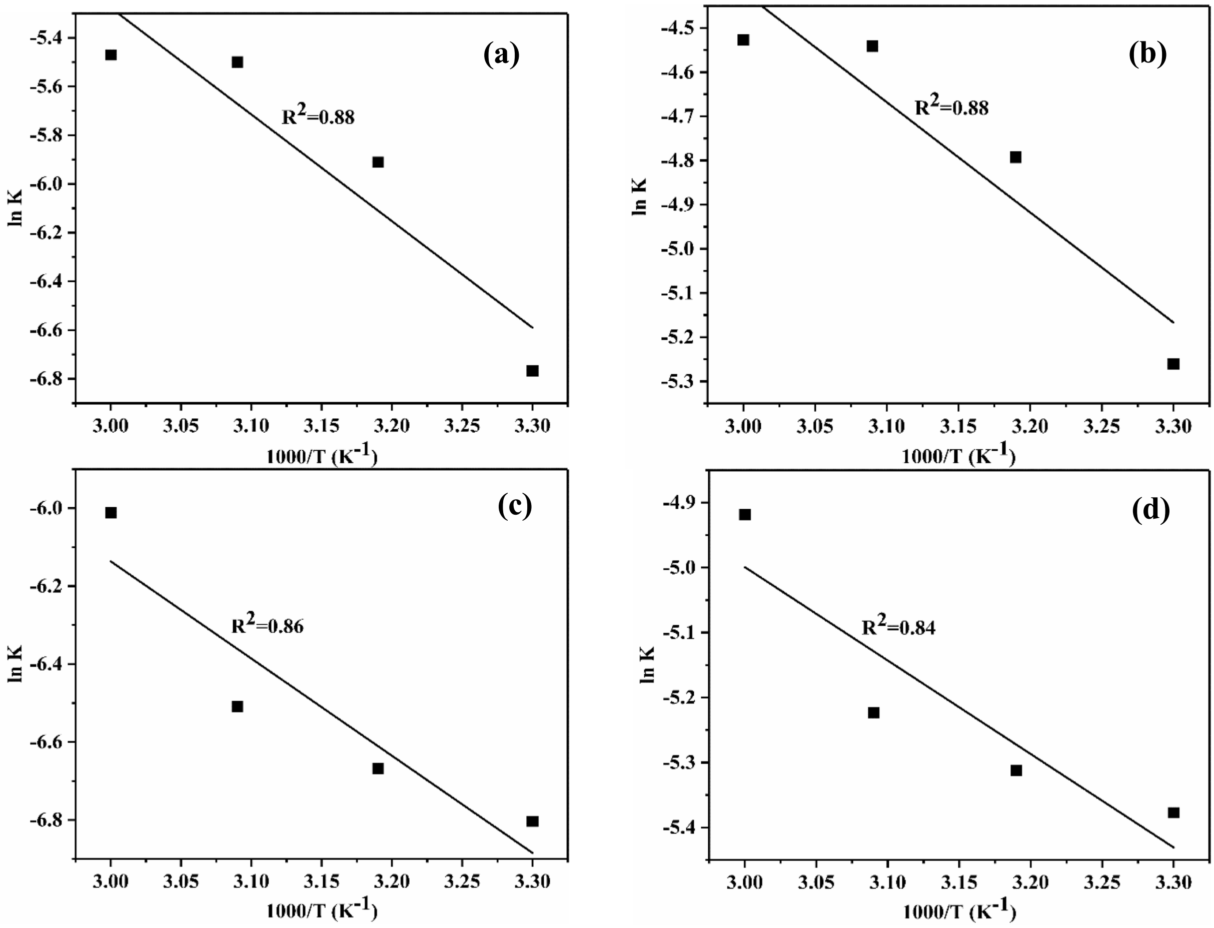

Figure 3.12 Arrhenius plot for leaching of copper for (a) diffusion-controlled model and (b) reaction-controlled model and leaching of zinc for (c) diffusion-controlled model and (d) reaction-controlled model

3.3. Conclusions

In this chapter, a hydrometallurgical approach was devised to achieve the highest possible retrieval of base metals such as copper and zinc from discarded printed circuit boards found in obsolete computer motherboards. The key findings from this chapter are outlined as follows:

- It is clear from the EDS and map of the cross-section of bare PCB that PCB has sandwich structure and is composed of five distinct layers:

(a) two solder mask layers (upper and lower layers) that is the top resin layer on soft-woven fiberglass to protect the circuit from corrosion; predominantly of Si and Ba

(b) two metal layers (upper and lower layer) predominantly made of copper foil and a coating of Sn, Ni, Zn, Ag on the surface of copper layers

(c) the polymer substrate layer made of brominated epoxy resin, reinforcing material made of glass fiber (composed of SiO_2, Al_2O_3, CaO, MgO, BaO etc.). All the layers of PCB were glued together by brominated epoxy resin.

- The XRD pattern of metal foil liberated after delamination of PCBs indicates the presence of copper.
- A metal leaching process that selectively dissolves copper, zinc, and nickel to leave a tin-rich solid residue has been successfully demonstrated.
- Optimal conditions for maximum leaching were 3 M nitric acid at 30°C, 2 h time period, for 50 g/L pulp density, and 500 rpm agitation speed. Leaching efficiency of 99.9% and 99.3% is obtained for copper and zinc respectively at optimal conditions.
- Chemical analysis of the filtered leach solution at the optimized parameters revealed that it comprises of 98±1 wt% copper, 0.57±0.1 wt% zinc, along with minor quantity of nickel.
- Kinetic studies show that the activation energies calculated for copper and zinc dissolution lie in the mixed mechanism mode of dissolution.